International Journal on Emerging Technologies 11(5): 85-89(2020)

ISSN No. (Print): 0975-8364
ISSN No. (Online): 2249-3255

Determination of Alumina Content during Aluminum Electrolysis in Cryolite-Alumina Melts

O.Yu. Tkacheva[1], P.A. Arkhipov[1], Yu. P. Zaikov[2] and A.M. Ivanova[3]
[1]Leading Scientist, Institute of High Temperature Electrochemistry, Yekaterinburg, Russia.
[2]Scientific Director, Institute of High Temperature Electrochemistry, Yekaterinburg, Russia.
[3]Head of the Scientific and Technical Center Elter, Krasnoyarsk, Russia.

(Corresponding author: O. Yu. Tkacheva)
(Received 03 June 2020, Revised 03 July 2020, Accepted 18 July 2020)
(Published by Research Trend, Website: www.researchtrend.net)

ABSTRACT: In order to develop a strategy of alumina supplying the electrolysis cell, a change of the alumina content dissolved in cryolite electrolyte during long-term aluminum electrolysis was studied under different modes of alumina feeding. The experiment was carried out using a lab setup providing the electrolyte convection due to the anode gas evolution. The electrolyte composition was close to the conventional one: NaF-AlF_3 with CR=2.7, CaF_2 5 wt%. The initial content of Al_2O_3 in the electrolyte was 4 wt%. The electrolyte samples were withdrawn during electrolysis in order to determine the Al_2O_3 content by means of an Oxygen Analyzer. The alumina dissolution rate in the electrolyte was found by comparing the values of the dissolved alumina content, determined in the electrolyte sample, and the loss of alumina consumed in the electrochemical reaction of the aluminum production. Measurements of the side ledge thickness formed due to solidification of the electrolyte during electrolysis were conducted. Under the conditions of electrolysis, at a rate of the alumina addition of 10 g/h, 36% of the added alumina was spent on increasing the alumina content in the melt; 44.6% was depleted on the electrochemical reaction; 19.4% did not dissolve in the electrolyte, but was involved in the formation of the side ledge. Thus, the content of dissolved alumina in the electrolyte increased and the side ledge was observed, which indicated an incorrect mode of the alumina supply. A decrease in the alumina feeding rate to an average value of 5.88 g/h contributed to the stabilization of electrolysis. In this case the side ledge was not formed and the content of dissolved alumina in the melt was constituted during electrolysis. That is, the conditions for optimal alumina feeding have been found for the electrolysis process under studied conditions.

Keywords: Alumina, aluminum electrolysis, cryolite, dissolution, feeding rate, side ledge

Abbreviations: CR, cryolite ratio.

I. INTRODUCTION

The processes of mass and heat transfer in industrial aluminum cells have a significant impact on the technological parameters and technical and economic indicators of their operation [1-3]. These processes are determined, first of all, by hydrodynamic flows in cryolite-alumina melt and liquid aluminum. Moreover, the role of hydrodynamic processes increases sharply with an increase in the size and power of reduction cells [4]. Hydrodynamic flows in the melt effect such important mass transfer processes as the dissolution and transport of alumina from the bulk, located between the cell wall and the anode (dissolution zone), to the pole gap (consumption zone); the equalization of the melt constituents concentrations; the formation of the working space in the cell (formation of a side and bottom ledge). Analysis of the experimental data [5] revealed that the interelectrode space can be divided into two regions, differing in the alumina content: near anode - with low alumina concentration and central - with high alumina concentration. The near-anode region corresponds to a zone with the movement of a melt depleted in Al_2O_3 under the influence of natural convection forces and floating bubbles of anode gas. The central region corresponds to a zone in which the intense mixing of the melt takes place by floating large gas bubbles.

Recently, a fairly large number of works, devoted to the study of the processes of the alumina dissolution and distribution in an electrolytic cell have been published [6-12]. Summarizing the results, the alumina dissolution process can be separated into several stages:

1) the alumina is distributed over the surface of the electrolyte and heats up, which leads to freezing of the electrolyte around the alumina particles. If there is insufficient heat, freezing becomes long, and a dense, insoluble crust forms;
2) when heated, the alumina crystals located in the middle are transformed into α-modification, and a sintering of alumina particles occurs;
3) when the frozen formations finally melt, the alumina granules can form agglomerates or lumps, that sink in the electrolyte;
4) the chemical interaction of alumina with molten cryolite begins as soon as the alumina enters the electrolyte bath. In this case, oxyfluorides are formed, diffusing deep into the melt.

The authors [12] determined the main parameters increasing the alumina dissolution rate: the maximum concentration of cryolite ions in the electrolyte, therefore, a tendency towards an increase in the CR; the lowest initial concentration of dissolved alumina in

the electrolyte; maximum available electrolyte surface; maximum rate of heat transfer to the liquid surface and maximum mass transfer of products.

In general, researchers agree that the parameters of dissolution and monitoring the alumina concentration in the cell during electrolysis cannot be studied under industrial conditions [13-15].

The authors [13] developed a setup for determining the parameters of the alumina dissolution in cryolite melt using a lab installation, which allowed the alumina concentration to be measured after 2 seconds with an accuracy of 10%. It was possible to load from 0.2 to 0.6 kg of electrolyte into the installation. The first stage of dissolution, as also reported in [5], proceeded very quickly (in 10 s). The remainder of the alumina dissolved much more slowly due to the formation of agglomerates. In this case, the contact surface of the electrolyte with alumina was significantly reduced. And in the second stage, the dissolution rate changed by 8 times, which could not be explained only by mass transfer since the melt was far from saturation.

If the dissolution time is significantly increased, then there is a risk of sludge formation and, consequently, an unfavorable electrolysis mode [5, 16, 17].

The mechanism of the side ledge formation is described in works [18-24]. The authors [18] put forward a "three-zone theory" of the side ledge structure. According to which the zone closest to the cold wall of the cell consists of sodium (mainly) and calcium cryolites, without alumina; the middle zone, the so-called open crystalline layer, includes dendrites, columnar disordered crystals of the same composition as the previous zone, but they are surrounded by a liquid electrolyte with a lower CR than the main electrolyte, close in composition to chiolite, in the same zone it was identified alumina as an individual phase; the third compressed (closed) layer is formed near the solid-liquid interface due to more active mass transfer with the electrolyte. The structure of the zones varies with a change in the heat flow due to the melting or crystallization of the open crystalline layer.

Extensive studies devoted to the mechanism of the formation of solid deposits at the cathode were carried out by researchers [5, 25, 26]. The purpose of work [26] was to determine the effect of the alumina feeding rate and the temperature gradient on the composition of the deposits at the cathode. It is mentioned, that these deposits limit the cathode area, which leads to a decrease in the current flow and an increase in the cell instability. The deposits can be in solid or solid-liquid state. The proportion of alumina in them changes from 20 to 50 wt%. It was concluded that to minimize energy consumption, the electrolysis cell should operate at a lower voltage. But at the same time, the overheating becomes less, the ledge is thicker, and more solid deposits appear on the cathode. Thus, the formation of solid deposits on the cathode is a consequence of two phenomena: dissolution and deposition of alumina, and heat losses on the cathode surface.

Sludge formation as a result of the slow alumina dissolution is undesirable, as it violates the power current lines and lowers the current efficiency. In turn, large changes in the alumina content lead to an increase in the frequency of anode effects.

Thus, the efficient dissolution of alumina is a critical factor in stable aluminum electrolysis. Fast alumina dissolution is achieved if a large mass of alumina is well distributed in the electrolyte and the resulting agglomerates quickly decompose. The anode gas evolution increases the dissolution rate, facilitating the dispersion of the alumina granules as well as the disintegration of agglomerates.

Various technological procedures aimed at improving the rate of alumina dissolution in the electrolyte and its distribution over the bath are widely applied in the aluminum industry. Such techniques include the use of automatic alumina feed, point feeding, reduction of electrolyte volume, etc [27-29].

In order to minimize the problem of dissolution and distribution of alumina in an industrial cell, a complex of technological improvements is required, aimed at adapting the cell by changing the operating parameters (electrolyte composition, alumina feeding strategy, overheating, operating temperature) in accordance with the quality of alumina [29].

The purpose of the work was to determine the alumina content in the electrolyte of conventional composition and the alumina distribution in the cell during aluminum electrolysis under different conditions of the alumina feeding (frequency and amount).

II. MATERIALS AND METHODS

The aluminum electrolysis was carried out in the cryolite electrolyte of the conventional composition, consisting of NaF (57 wt%), AlF_3 (49 wt%) and CaF_2 (5 wt%), CR 2.7. The electrolyte was prepared from individual salts NaF and AlF_3(both supplied by Vekton, RF). The initial alumina content in the electrolyte was 4 wt%. The X-ray phase analysis and particle size analysis of the alumina Al_2O_3 (Granchim, RF)revealed that it contained 27.3% α-Al_2O_3, 60.7% γ-Al_2O_3, 12.1% η-Al_2O_3 with an average particle size of 60 μm.

The experimental measurements of the alumina content in cryolite are based on the principle of creating electrolysis conditions that are as close as possible to processes occurring in existing electrolysis cells. For this, a sufficient volume of electrolyte is needed, so that the alumina content in the electrolyte is determined not only by natural convection, but also by forced convection resulting from anode gas evolution during electrolysis.

The electrolysis was carried out in a lab setup, schematically depicted in Fig. 1. A graphite crucible filled with electrolyte and aluminum at the bottom was placed in a protective steel container. The cell was installed using the lifting mechanism in the furnace. A cover with a heat insulator closed the furnace shaft.

The operating parameters of aluminum electrolysis were as follows: current 13,7÷14,8 A; electrolyte temperature 980℃; the anode current density 0,75 A/cm^2. The aluminum level in the crucible was about 80 mm; the electrolyte mass was about 10 kg; the electrolyte level was 140÷160 mm; the interpolar distance was 30 mm, and the electrolysis elapsed time was about 60 h.

The mass of each alumina addition (m) to the electrolyte during electrolysis was determined by the equation:

$$m = E \cdot I \cdot t \cdot 1.89 \quad (1)$$

where E is the electrochemical equivalent, I is the current, t is the electrolysis time. The conversion factor of aluminum metal into alumina is 1.89.

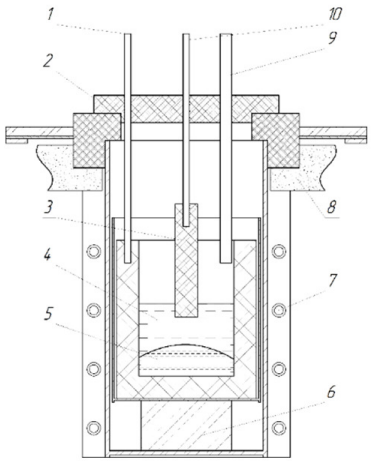

Fig. 1. Electrolysis cell schematic: 1. current lead to graphite crucible served as a cathode, 2. cover with mounted holes for current leads and tube for alumina adding and sampling, 3. graphite anode, 4. electrolyte, 5. liquid aluminum, 6. fire-clay brick, 7. furnace, 8. lining.

The rate of adding alumina $u(Al_2O_3)$ in the electrolyte is determined as:

$$u(Al_2O_3) = \sum m_i / \Delta t \quad (2)$$

where m_i is the mass of alumina added after a certain period of time Δt.

Measurements of the side ledge thickness, formed during the solidification of the electrolyte for the period of electrolysis, were conducted by the measuring mechanism. It was mounted on a platform with a ruler. The thickness was determined by the difference between the measurement before electrolysis and during electrolysis. The procedure is described in more detail elsewhere [30].

The electrolyte samples were withdrawn during electrolysis in order to determine the alumina content. The oxygen analysis was performed using an ELTRA ON 900 Oxygen Analyzer.

The alumina dissolution rate in the electrolyte was found by comparing the values of the dissolved alumina content, determined in the electrolyte sample, and the loss of alumina consumed in the electrochemical reaction.

III. RESULTS AND DISCUSSION

A voltage change during electrolysis is given in Fig. 2. Voltage dips are associated with the current disconnection, during which the thickness of the side ledge was measured and samples of electrolyte was taken for chemical analysis.

The mass of the alumina addition calculated according to Faraday's law, taking into account 50% of current efficiency, was 4.5 g per hour. A frequency of alumina additions to the electrolyte during the entire electrolysis is presented in Fig. 2. The alumina was not added during the first 7 h of electrolysis, while the voltage reached a constant value of 2.2 V. From the 7th to 11th h, thealumina in amount of 4.5 g/h was added; however, the voltage did not reach the technological value of 2.5 B.

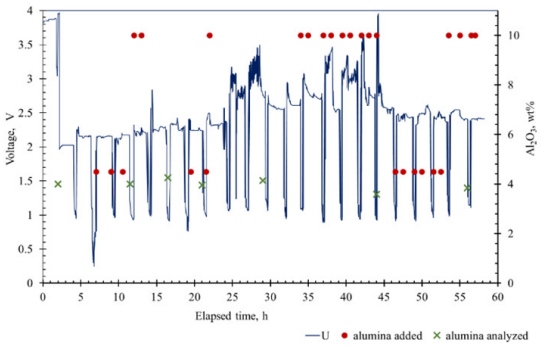

Fig. 2. The cell voltage, the amount and frequency of alumina additions, and the analyzed alumina content in the electrolyte during electrolysis.

The alumina content in the electrolyte decreased to 3.96% by 19th h. Therefore, the mass of addition was increased to 10 g (at 22 h). However, at 24th hour of the process, the electrolyte temperature decreased, and the voltage fluctuation began. The heat losses were reduced by additional insulation of the furnace with lining material. It helped to stabilize the voltage (at 30th h). Then, with the addition of 10 g/h, the voltage fluctuation stopped. The alumina content in the electrolyte increased from 3.59% to 3.85% and it was 3.81% by the end of the experiment.

The side ledge profile along the crucible height formed during long-term electrolysis is plotted in Fig.3. The side ledge was not produced during the first 10 h. Analysis of the electrolyte sample withdrawn after 10 h of electrolysis showed that the alumina content remained unchanged (4.09% and 4.08%). This proves that all the alumina supplied in doses of 4.5 g per hour was dissolved and spent on the electrochemical reaction to produce aluminum.

From 12th h, the dose of adding was increased to 10 g/h. At constant temperatures and CR, an almost 2-fold increase in the dose of alumina resulted in the formation of the side ledge. Chemical analysis of the electrolyte on alumina gave 4.26 wt%.

The rate of the alumina addition during the period from 11 to 16 h of electrolysis calculated according to eq. (2) was 10 g/h. It was added 50 g Al_2O_3. Of these, the consumption of alumina due to electrolysis at an average current of 14.8 A and a current efficiency of 50% amounted to 22.3 g; another 18 g was consumed to increase the alumina content from 4.07 to 4.26%; the remaining 9.7 g (19.4%) of the alumina went into solid precipitate to form a side ledge, the thickness of which increased from 2 to 12 mm. Thus, at the rate of 10 g/h, about 19.4% of the added alumina does not have time to dissolve in the electrolyte. The undissolved alumina, due to convective flows created by active gas evolution at the anode, is transferred to the walls of the cell and settles. By the end of the electrolysis, the formed side ledge is almost unchanged. Therefore, the dissolution rate of alumina is determined only by its soluble part, in other words, all incoming alumina into the melt goes into the active electrochemical form and is spent on the production of aluminum metal.

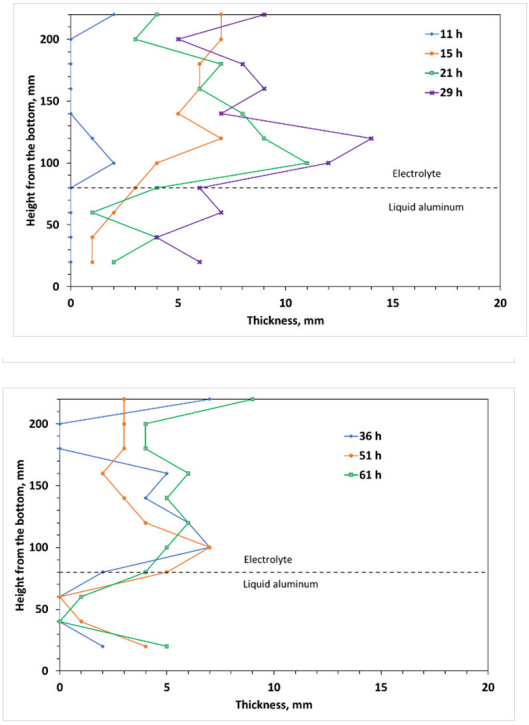

Fig. 3. Side ledge profile formed during long-term electrolysis in the lab cell

The rate of adding alumina, determined during the period from the 36th to the 61st h of electrolysis, amounted to 5.88 g/h. The alumina content in the electrolyte analyzed at the end of the electrolysis was 3.85 wt% (56th h) and 3.81 wt% (61st h). The constancy of the alumina content in the electrolyte confirms the optimal rate of alumina addition.

IV. CONCLUSION

The experimental measurements of the alumina content in cryolite electrolyte were carried out during electrolysis in a lab cell. The electrolyte composition was close to conventional one:NaF-AlF_3(CR 2.7), CaF_2(5 wt%), Al_2O_3 4 wt%. The initial temperature of electrolysis was 980 ºC. Electrolysis conditions provided the forced mixing of the electrolyte due to the anode gas evolution. It was found that at a rate of the alumina feeding 10 g/h, 36% of the added alumina is spent on increasing the alumina content in the melt; 44.6% is spent on the electrochemical reaction; 19.4% does not dissolve in the electrolyte, but is involved in the formation of the side ledge. Thus, at the alumina feeding rate of 10 g/h, the content of dissolved alumina in the electrolyte increases and the side and bottom ledge are formed, which indicates an incorrect mode of the alumina supply to the cell. A decrease in the rate of alumina addition to an average value of 5.88 g/h contributed to the stabilization of electrolysis. The formation of ledge was not observed and the content of dissolved alumina in the melt was constituted during electrolysis. That is, the conditions for optimal alumina feeding have been found for the electrolysis process under studied conditions.

V. FUTURE SCOPE

The obtained results regarding the alumina content in cryolite melt during aluminum electrolysis can be used for developing criteria for the dissolution and distribution of alumina in an industrial electrolyte, which can be applied as boundary conditions in a predictive mathematical model of the dissolution and distribution of alumina. Based on this model, the optimal alumina feeding system for industrial electrolysis cell will be established.

ACKNOWLEDGEMENT

This work has been financially supported by the Ministry of Education and Science of RF under the federal target program (Agreement EB N075-15-2019-1949, internal N05.604.21.0239, IN RFMEFI60419X0239).

Conflict of Interest. No.

REFERENCES

[1]. Lavoie, P., Nailor, M.P., & Metson J.B. (2016). A review of alumina feeding and dissolution factors in aluminum reduction cell. *Met. Mat. Trans. B.*, *47*: 2690-2696.
[2]. Grotheim, K., Kvande, H. (1993). Introduction to Aluminium Electrolysis: Understanding the Hall-Hérloult process. Dusseldorf: Aluminium-Verlag: 61-87.
[3]. Solheim, A., (2011). Some aspects of heat transfer between bath and side ledge in aluminum production. *TMS Light Metals 2011*: 381-386.
[4]. Oye, H. A., Mason, N., Peterson, R.D., & Richards, N. E. (1999). Aluminium: Approaching the new millennium. *JOM*, *51*: 29-42.
[5]. Solheim, A. (2006). Towards the proper understanding of sideledge facing the metal in aluminum cells? *TMS Light Metals 2006*: 439-444.
[6]. Rain, R.K., Tricklebank, S.B., Welch, B.J., Williams, D.J., (1983). Interaction of alumina with aluminium smelting electrolytes. *TMS Light Metals 1983:* 609-622.
[7]. Kobbeltvedt, O., Rolseth, S., & Thonstad, J. (1996). On the mechanism of alumina dissolution with relevance to point feeding aluminum cells. *TMS Light Metals 1996*: 421-427.
[8]. Kaszas, C., Kiss, L., Guerard, S., Bilodeau, & J. F., (2015). Behaviour of powders on the surface of a liquid.*TMS Light Metals 2015*.Springer, Cham: 639-642.
[9]. Gylver, S. E., Omdahl, N.H., Prytz, A.K., Meyer, A.J., Lossius, L.P., & Einarsrud K.E. (2019). Alumina feeding and raft formation: Raft collection and process parameters. *Light Metals 2019, The Minerals, Metals & Materials Series,* Springer, Cham: 659-666.
[10]. Dando, N., Wang, X., Sorensen, J., Xu, W.,(2010). Impact of thermal pretreatment on alumina dissolution rate and HF evolution. *TMS Light Metals 2010*: 541-546.
[11]. Lindsay, S.J. Key physical properties of smelter grade alumina. *TMS Light Metals 2014*, Springer, Cham: 597-602.
[12]. Skybakmoen, E., Solheim, A., & Sterten, A. (2016). Liquidus temperature and alumina solubility in the system Na_3AlF_6-AlF_3-LiF-CaF_2-MgF_2, *Essential Readings in Light Metals, Aluminum Reduction Technology*, 2, Springer: 73-79.

[13]. Welch, B.J., & Kuschel, G.I. (2007). Crust and alumina powder dissolution in aluminum smelting electrolytes. *JOM*, *59*: 50-54.
[14]. Kuschel, G.I., & Welch, B.J. (1991). Further studies of alumina dissolution under conditions similar to cell operation. *TMS Light Metals,* 112-118.
[15]. Liu, X., George, S.F., & Wills, V.A. (1994). Visualization of alumina dissolution in cryolitic melts, *TMS Light Metals 1994:* 259-364.
[16]. Liu, J., Wei, S., & Taylor, M. (2019). The structure of the smelting cell ledge under variable sidewall heat flow conditions. *JOM*, *71*(2): 514-521.
[17]. Rudenko, A. V., Kataev, A. A., Tkacheva, O. Yu., Red'kin, A. A., and Zaikov Yu. P., (2019). Electrical conductivities of solid and liquid cryolite systems. *Russian Metallurgy (Metally)*, 104–107.
[18]. Allard, F., Soucy, G., & Rivoaland, L. (2014). Cartography and chemical composition of the different deposits in the Hall-Heroult process. *TMS Light Metals 2014*, Springer, Cham: 1233-1238.
[19]. Liu, J., Fallan-Mehrjardi, A., Shishin, D., Jak, E., Dorreen, M., Taylor, M., (2017). Investigation of the influence of heat balance shifts on the freeze microstructure and composition in aluminum smelting bath system: cryolite-CaF_2-AlF_3-Al_2O_3. *Met. Mat. Trans. B.*, *46*: 3185-3195.
[20]. Kiss, L., & Dassylva-Raymond, V., (2008). Freeze thickness in aluminum electrolysis cell. *TMS Light Metals*: 431-436.
[21]. Marois, M., Bertrand, C., Deselets, M., Coulombe, M., & Lacroix M. (2009). Comparison of two different numerical methods for predicting the formation of the side ledge in an aluminum electrolysis cell. *TMS Light Metals:* 563-568.
[22]. Yasinskiy, A., Polyakov, P., Voyshel, Y.V., Glimanshina, T.R., & Padamata, S.K. (2018). Sedimentation behavior of high-temperature concentrated colloidal suspension based on potassium cryolite. *J. Dispersion Science and Technology, 39*(10): 1492-1501.
[23]. Azema, N. (2006). Sedimentation behavior study by three optical method – granulomentric and electrophoresis measurements? Dispersion optical analyzer. *Powder technology*, *165*: 133-139.
[24]. Liu, J.,Wei, S., Chen, J.J., Wijayarathe, H., Wang, Z., Gao, B., & Taylor M. (2020). Investigation of the ledge structure in aluminum smelting cells. *JOM*, *72*: 253-262.
[25]. Allard, F., Soucy, G., & Rivoaland, L. (2014). Formation of deposits on the cathode surface of aluminum electrolysis cell. *Met. Mat. Trans., B*, *45*: 2475-2491.
[26]. Allard, F., Soucy, G., Rivoaland, L., and Desilets, M., (2015). Thermodynamic and thermochemical investigation of the deposits. *J. Therm. Anal. Calorim., 119*: 1303–1314.
[27]. Tonstad, J., Fellner, P., Haarberg, G.M., Hives, J., Kvande, H., & Sterten A. (2005). Aluminum electrolysis. Fundamentals of the Hall-Heroult process. 3rd ed. Aluminium-Verlag: 272-292.
[28]. Thonstad, J., Johansen, P., & Kristensen, E.W. (1980). Some properties of alumina sludge. *Light Metals 1980*: 227-239.
[29]. Buzunov, V. Yu., Pecherskaya, T.D., Tayanchin, A.S., & Chesnyak, V.V. (2013). The impact of alumina quality on the performance of smelting, *Proceedings of the Vth International Congress, Aluminium of Siberia - 2013,* Krasnoyarsk, Russia: 753-761.
[30]. Tkacheva, O., Arkhipov, P., & Zaykov, Yu., (2020). Solid phase formation during aluminum electrolysis. *Electrochemistry communications, 110*: 106624-9.

How to cite this article: Tkacheva, O. Y., Arkhipov, P. A., Zaikov, Y. P. and Ivanova, A. M. (2020). Determination of Alumina Content During Aluminum Electrolysis in Cryolite-Alumina Melts. *International Journal on Emerging Technologies, 11*(5): 85–89.